High order volume-preserving algorithms for relativistic charged particles in general electromagnetic fields

Cite as: Phys. Plasmas **23**, 092109 (2016); https://doi.org/10.1063/1.4962677
Submitted: 24 June 2016 . Accepted: 30 August 2016 . Published Online: 20 September 2016

Yang He, Yajuan Sun, Ruili Zhang, Yulei Wang, Jian Liu, and Hong Qin

High order volume-preserving algorithms for relativistic charged particles in general electromagnetic fields

Yang He,[1] Yajuan Sun,[2,3] Ruili Zhang,[4,5] Yulei Wang,[4,5] Jian Liu,[4,5] and Hong Qin[4,6]
[1]*School of Mathematics and Physics, University of Science and Technology Beijing, Beijing 100083, China*
[2]*LSEC, Academy of Mathematics and Systems Science, Chinese Academy of Sciences, P.O. Box 2719, Beijing 100190, China*
[3]*University of Chinese Academy of Sciences, Beijing 100049, China*
[4]*Department of Modern Physics and Collaborative Innovation Center for Advanced Fusion Energy and Plasma Sciences, University of Science and Technology of China, Hefei, Anhui 230026, China*
[5]*Key Laboratory of Geospace Environment, CAS, Hefei, Anhui 230026, China*
[6]*Plasma Physics Laboratory, Princeton University, Princeton, New Jersey 08543, USA*

(Received 24 June 2016; accepted 30 August 2016; published online 20 September 2016)

We construct high order symmetric volume-preserving methods for the relativistic dynamics of a charged particle by the splitting technique with processing. By expanding the phase space to include the time t, we give a more general construction of volume-preserving methods that can be applied to systems with time-dependent electromagnetic fields. The newly derived methods provide numerical solutions with good accuracy and conservative properties over long time of simulation. Furthermore, because of the use of an accuracy-enhancing processing technique, the explicit methods obtain high-order accuracy and are more efficient than the methods derived from standard compositions. The results are verified by the numerical experiments. Linear stability analysis of the methods shows that the high order processed method allows larger time step size in numerical integrations. *Published by AIP Publishing.* [http://dx.doi.org/10.1063/1.4962677]

I. INTRODUCTION

The dynamics of relativistic particles under the influence of electromagnetic fields is a fundamental process in plasma physics, space physics, accelerator physics, etc. Numerical simulations on trajectories of charged particles have been widely used to study their dynamical behaviours. In most multi-scale problems, such as runaway electron dynamics in tokamaks and the formation of energetic electrons in the magnetosphere, long-term numerical integrations are required to reproduce the entire physical processes. For example, in tokamaks, the typical timescale of the runaway acceleration process is about 1 s, which is 10^8 times larger than its transit period. It is thus essential for the numerical algorithms to be accurate and fast over long time in tracking the secular particle trajectory. Conventional methods such as the fourth order Runge-Kutta method, though with a fourth order of accuracy in each step, often fail to trace the correct trajectory after a long time of computation due to the error accumulation. One way to overcome this difficulty is to apply geometric integration methods.[1–4] By preserving the intrinsic structures of the dynamical system, geometric integration methods usually generate numerical results with better accuracy and conservative properties, which have been proven theoretically.[4,5] Recently, following the idea of geometric integration, a series of advanced algorithms have been developed for the long-term accurate simulations of charged particle dynamics and Vlasov-Maxwell systems.[6–22] In Refs. 12 and 13, for the non-relativistic dynamics of a charged particle, we have presented the geometric integration methods based on its volume-preserving property. In this paper, we further develop the idea to study the charged particle dynamics with relativistic effects.

The relativistic dynamics of a charged particle in the electromagnetic fields $\mathbf{E}$ and $\mathbf{B}$ are governed by

$$\begin{aligned} \frac{d\mathbf{x}}{dt} &= \frac{1}{m_0\gamma(p)}\mathbf{p}, \\ \frac{d\mathbf{p}}{dt} &= q\mathbf{E}(\mathbf{x},t) + \frac{q}{m_0\gamma(p)}\mathbf{p}\times\mathbf{B}(\mathbf{x},t), \end{aligned} \tag{1}$$

where $\mathbf{x}$ and $\mathbf{p}$ are the position and momentum vectors, m_0 and q denote the rest mass and charge of the particle, and $\gamma(p)=\sqrt{1+p^2/(m_0^2c^2)}$ is the Lorentz factor with c the speed of light in vacuum. Let $p/c\to 0$, we notice that Eq. (1) leads to a non-relativistic Lorentz force equation. Although the physical nature of the relativistic system is different from the non-relativistic system, they have similar geometric structures. For example, the system (1) is still source-free with

$$\nabla_{\mathbf{z}}\cdot\mathbf{F}(\mathbf{z}) \equiv \nabla_{\mathbf{x}}\cdot\left(\frac{\mathbf{p}}{m_0\gamma(p)}\right) + \nabla_{\mathbf{z}} \cdot\left(q\mathbf{E}(\mathbf{x},t)+\frac{q\mathbf{p}\times\mathbf{B}(\mathbf{x},t)}{m_0\gamma(p)}\right)=0,$$

and the solution is volume-preserving.[12,14,22] Based on the volume-conserving structure of the motion equations, symmetric volume-preserving (SVP) algorithms have been proposed for solving the secular relativistic[14] and non-relativistic[11–13] dynamics of a charged particle. One of the major properties of these algorithms is that the volume form in phase space $(\mathbf{x}, \mathbf{p})$ is invariable along the numerical solution mapping $\phi_h : (\mathbf{x}_k, \mathbf{p}_k)\mapsto(\mathbf{x}_{k+1}, \mathbf{p}_{k+1})$, which implies the following equation:

$$\det\left(\frac{\partial(\mathbf{x}_{k+1},\mathbf{p}_{k+1})}{\partial(\mathbf{x}_k,\mathbf{p}_k)}\right)\equiv 1.$$

Another property is that the methods are time-symmetric, that is, $\phi_h=\phi_{-h}^{-1}$. It has been performed numerically that the SVP methods can guarantee the long-term accuracy of numerical solutions and the conservation of the constants of motion such as energy and angular momentum. Moreover, they can be iterated explicitly and implemented easily, thus are efficient in solving the secular trajectories of charged particles. Thus, these methods have potentials to be developed as particle solvers in Particle-In-Cell (PIC) codes.[23]

In the current paper, we present explicit, high order symmetric volume-preserving algorithms for the relativistic dynamics under the general electromagnetic fields. It is pointed out in Refs. 11 and 24 that numerical methods maintaining the volume-preserving property can be derived by using the splitting technique. By investigation, we notice that the Equation (1) can be decomposed as a summation of three source-free subsystems. Thus, SVP methods can be constructed by symmetric compositions of the volume-preserving update mappings that solve the corresponding subsystems. However, when the electromagnetic fields are time-dependent, it is not always trivial to solve the subsystems exactly. Therefore, we expand the phase space by appending the time t to the dependent variables. It follows that the non-autonomous system is turned into an autonomous system. We prove that the new system is source-free and can be split into exactly solvable subsystems; thus, SVP methods are constructed for system (1) even with time-dependent electromagnetic field.

As the SVP methods are developed using the splitting technique, it is clear that the higher the order of accuracy is, the larger number of composition mappings is required. This leads to a large computational expense in numerical simulations. To reduce the computation cost over the simulation interval, we employ the accuracy-enhancing processing technique[25,26] to construct the method in the form $\tilde{\Psi}_h=\chi_h\circ\Psi_h\circ\chi_h^{-1}$. In this method, the kernel Ψ_h is a one step method for the system, the processor χ_h is a near identity map, and $\circ$ denotes the composition operation. Theoretically, the method $\tilde{\Psi}_h$ can be constructed to achieve arbitrarily high-order of accuracy, as long as the order conditions are satisfied by the kernel and the processor.[25,26] After N steps of iteration, there is $\tilde{\Psi}_h^N=\chi_h\circ\Psi_h^N\circ\chi_h^{-1}$. From the relation, it is easy to see that the computing efforts of $\tilde{\Psi}_h^N$ mainly come from Ψ_h^N for large N. A most efficient method can be derived by choosing the kernel method Ψ_h as simple as possible, and searching for the processor χ_h to achieve the desired order of accuracy. For the non-relativistic dynamical systems,[13] the efficiency of this kind of methods has been verified. In this paper, for the relativistic dynamics, we split the motion equations as three parts and develop efficient high order SVP methods by applying the processing technique. We analyze the linear stability of the numerical methods and show the numerical experiments. It claims that the newly derived high order methods are more efficient than the conventional composition methods and allow a larger step size according to the stability conditions.

This paper is organized as follows. In Section II, we derive SVP methods for the relativistic dynamical systems with general time-dependent electromagnetic fields by using the splitting and processing technique. In Section III, we present the study of the linear stability for the SVP methods. In Section IV, the newly developed SVP methods are tested by two physical problems: the penning trap and the problem possessing a plane polarized electromagnetic wave.

II. HIGH ORDER VOLUME-PRESERVING ALGORITHMS

In this section, we give a general derivation of high order volume-preserving algorithms for simulating the relativistic orbits under a time-dependent electromagnetic field, by using the splitting and accuracy-enhancing processing technique.

We consider the most general case in which the electromagnetic fields are time-dependent. To apply the splitting and processing technique, we introduce $\sigma=t$ as a new dependent variable, then it follows from (1) that

$$\frac{d}{dt}\begin{pmatrix}\mathbf{x}\\ \mathbf{p}\\ \sigma\end{pmatrix}=\begin{pmatrix}\dfrac{1}{m_0\gamma(p)}\mathbf{p}\\ q\mathbf{E}(\mathbf{x},\sigma)+\dfrac{q}{m_0\gamma(p)}\mathbf{p}\times\mathbf{B}(\mathbf{x},\sigma)\\ 1\end{pmatrix}. \tag{2}$$

From Eq. (2), it can be seen that with the coordinate ($\mathbf{x}$, $\mathbf{p}$, σ), the system (1) becomes an autonomous system which are defined in an expanded space $\mathbb{R}^3\times\mathbb{R}^3\times\mathbb{R}$ (see Ref. 27 for more details). We have shown before that the system (1) is source-free, and the exact solution is volume-preserving.[14] Notice that for any map $\Psi:(\mathbf{x},\mathbf{p},\sigma)\mapsto(\mathbf{X},\mathbf{P},\Sigma)$, if $\frac{\partial\Sigma}{\partial\mathbf{x}}=\frac{\partial\Sigma}{\partial\mathbf{p}}=\mathbf{0}$, $\frac{\partial\Sigma}{\partial\sigma}=1$, then its Jacobian satisfies

$$\det\left(\frac{\partial(\mathbf{X},\mathbf{P},\Sigma)}{\partial(\mathbf{x},\mathbf{p},\sigma)}\right)=\det\left(\frac{\partial(\mathbf{X},\mathbf{P})}{\partial(\mathbf{x},\mathbf{p})}\right).$$

Therefore, as long as the appended variable σ solves $\dot{\sigma}=const$, the expanded system (2) inherits the volume-preserving nature of the system (1). Similarly, the volume-preserving methods for the source-free system (2) in the expanded space also preserve the volume of phase space ($\mathbf{x}$, $\mathbf{p}$). This gives us a hint on how to split the system.

It is observed that the system (2) can be decomposed as three source-free solvable subsystems

$$\begin{aligned}\frac{d}{dt}\begin{pmatrix}\mathbf{x}\\ \mathbf{p}\\ \sigma\end{pmatrix}&=\begin{pmatrix}\dfrac{1}{m_0\gamma(p)}\mathbf{p}\\ 0\\ 1\end{pmatrix}+\begin{pmatrix}0\\ q\mathbf{E}(\mathbf{x},\sigma)\\ 0\end{pmatrix}\\&\quad+\begin{pmatrix}0\\ \dfrac{q}{m_0\gamma(p)}\mathbf{p}\times\mathbf{B}(\mathbf{x},\sigma)\\ 0\end{pmatrix}\\&=F_1(\mathbf{x},\mathbf{p},t)+F_2(\mathbf{x},\mathbf{p},t)+F_3(\mathbf{x},\mathbf{p},t).\end{aligned} \tag{3}$$

The first two subsystems with F_1 and F_2 can be solved exactly by a translational transformation as

$$\phi_h^{F_1}:\begin{cases}\mathbf{x}(t+h)=\mathbf{x}(t)+h\dfrac{\mathbf{p}(t)}{m_0\gamma(p(t))},\\ \mathbf{p}(t+h)=\mathbf{p}(t),\\ \sigma(t+h)=\sigma(t)+h,\end{cases}$$

$$\phi_h^{F_2}:\begin{cases}\mathbf{x}(t+h)=\mathbf{x}(t),\\ \mathbf{p}(t+h)=\mathbf{p}(t)+hq\mathbf{E}(\mathbf{x}(t),\sigma(t)),\\ \sigma(t+h)=\sigma(t).\end{cases}$$

Here, the mappings $\phi_h^{F_i}$, $i=1, 2, 3$ denote the h-time step updating. When the third subsystem is considered, it is noticed that $p^2=\mathbf{p}^\top\mathbf{p}$ is invariant along the exact solution flow, and therefore, so is $\gamma(p)$. Thus, the updating map $\phi_h^{F_3}$ of the exact solution can be calculated as

$$\phi_h^{F_3}:\begin{cases}\mathbf{x}(t+h)=\mathbf{x}(t), & (4a)\\ \mathbf{p}(t+h)=\exp\left(h\dfrac{q}{m_0\gamma(p(t))}\hat{\mathbf{B}}(\mathbf{x}(t),\sigma(t))\right)\mathbf{p}(t), & (4b)\\ \sigma(t+h)=\sigma(t), & (4c)\end{cases}$$

with $\hat{\mathbf{B}}=\begin{bmatrix}0 & B_3 & -B_2\\ -B_3 & 0 & B_1\\ B_2 & -B_1 & 0\end{bmatrix}$ defined by $\mathbf{B}(\mathbf{x})=[B_1(\mathbf{x}), B_2(\mathbf{x}), B_3(\mathbf{x})]^\top$. The operator exp in (4b) is the exponential operator of a matrix, which can be expressed in a closed form for a skew symmetric matrix of 3×3 as

$$\mathbf{p}(t+h)=\exp(ha\hat{\mathbf{B}})\mathbf{p}(t)=\mathbf{p}(t)+\frac{\sin(haB)}{B}\mathbf{p}(t)\times\mathbf{B}+\frac{(1-\cos(haB))}{B^2}\mathbf{p}(t)\times\mathbf{B}\times\mathbf{B}. \quad (5)$$

Here, $a=\frac{q}{m_0\gamma(p(t))}$.

It is easy to prove that each of the mappings $\varphi_h^{F_1}$, $\varphi_h^{F_2}$, $\varphi_h^{F_3}$ preserves the volume in phase space $(\mathbf{x}, \mathbf{p})$. Due to the group property, their various compositions provide the SVP methods of any order.[4,24,28] As follows, we present some SVP methods of second and fourth orders.

Second order symmetric methods. A second order symmetric method can be derived by the symmetric composition $G_h^2:=\phi_{\frac{h}{2}}^{F_1}\circ\phi_{\frac{h}{2}}^{F_2}\circ\phi_h^{F_3}\circ\phi_{\frac{h}{2}}^{F_2}\circ\phi_{\frac{h}{2}}^{F_1}$,

$$\begin{aligned}\mathbf{x}_{k+\frac12}&=\mathbf{x}_k+\frac{h}{2}\frac{\mathbf{p}_k}{m_0\gamma(p_k)},\\ \mathbf{p}^-&=\mathbf{p}_k+\frac{hq}{2}\mathbf{E}_{k+\frac12},\\ \mathbf{p}^+&=\exp\left(\frac{hq}{m_0\gamma(p^-)}\hat{\mathbf{B}}_{k+\frac12}\right)\mathbf{p}^-,\\ \mathbf{p}_{k+1}&=\mathbf{p}^+ +\frac{hq}{2}\mathbf{E}_{k+\frac12},\\ \mathbf{x}_{k+1}&=\mathbf{x}_{k+\frac12}+\frac{h}{2}\frac{\mathbf{p}_{k+1}}{m_0\gamma(p_{k+1})},\end{aligned} \quad (6)$$

where $\mathbf{E}_{k+\frac12}:=\mathbf{E}(\mathbf{x}_{k+\frac12},t_{k+\frac12})$, $\mathbf{B}_{k+\frac12}:=\mathbf{B}(\mathbf{x}_{k+\frac12},t_{k+\frac12})$ are the field values evaluated at the position $\mathbf{x}_{k+\frac12}$ and the time $t_{k+\frac12}$.

In the method G_h^2, we can replace $\phi_h^{F_3}$ with a numerical method $\Phi_h^{F_3}$ to the third subsystem, e.g., the midpoint method, then we get an alternative SVP method of the second order

$$\tilde{G}_h^2:=\phi_{\frac{h}{2}}^{F_1}\circ\phi_{\frac{h}{2}}^{F_2}\circ\Phi_h^{F_3}\circ\phi_{\frac{h}{2}}^{F_2}\circ\phi_{\frac{h}{2}}^{F_1}. \quad (7)$$

It recovers the numerical algorithm proposed in Ref. 14.

Higher order SVP methods can be derived via various compositions of approximate (exact) solutions of each subsystem. For example, a fourth order method can be derived by using the well known Yoshida's composition[29] as

$$G_h^4Y=G_{a_1h}^2\circ G_{a_2h}^2\circ G_{a_1h}^2, \quad (8)$$

or by using Suzuki's fourth order composition as[30]

$$G_h^4S=G_{b_1h}^2\circ G_{b_2h}^2\circ G_{b_3h}^2\circ G_{b_2h}^2\circ G_{b_1h}^2, \quad (9)$$

where $a_1=(2-2^{1/3})^{-1}, a_2=1-2a_1, b_1=b_2=(4-4^{1/3})^{-1}$, $b_3=1-2(b_1+b_2)$. In comparison, the method G_h^4S has a smaller error constant than the method G_h^4Y. It is clear from (8) and (9) that the higher order methods can produce numerical solutions of higher accuracy, but with larger computational expense. To reduce the computation cost, we then present efficient fourth order SVP methods by employing the accuracy-enhancing processing technique.

The main idea of the processing technique is to apply a near-identity transformation χ_h called the processor to a kernel integrator Ψ_h, such that the newly derived method $\tilde{\Psi}_h=\chi_h\circ\Psi_h\circ\chi_h^{-1}$ has a higher order of accuracy than Ψ_h. After N steps of iteration, there is $\tilde{\Psi}_h^N=\chi_h\circ\Psi_h^N\circ\chi_h^{-1}$. It states that $\tilde{\Psi}_h^N$ does not need more computational expense than Ψ_h^N. Moreover, $\tilde{\Psi}_h$ can effectively maintain all global properties (e.g., the long-term stability, structure-preserving property) inherited by the lower order method Ψ_h. For the relativistic dynamical system (1) with the splitting (3), the kernel and processor are given by the compositions of $G_h=\phi_h^1\circ\phi_h^2\circ\phi_h^3$ and $G_h^*=\phi_h^3\circ\phi_h^2\circ\phi_h^1$ as

$$\begin{aligned}\Psi_h&=G_{a_1h}\circ G_{b_1h}^*\circ G_{a_2h}\circ G_{b_2h}^*\circ\ldots\circ G_{a_sh}\circ G_{b_sh}^*,\\ \chi_h&=G_{x_1h}\circ G_{y_1h}^*\circ G_{x_2h}\circ G_{y_2h}^*\circ\ldots\circ G_{x_mh}\circ G_{y_mh}^*,\end{aligned} \quad (10)$$

where $\{a_i,b_i\}_{i=1}^s$ and $\{x_i,y_i\}_{i=1}^m$ are the composition coefficients determined by the order conditions.[26] As follows, we list a fourth order processed method whose coefficients are given in Ref. 26.

Fourth order symmetric methods. One of the processed composition methods reads

$$G_h^4P=\chi_h\circ\Psi_h\circ\chi_h^{-1}, \quad (11)$$

where Ψ_h and χ_h are in the form (10) with $s=m=4$, and the composition coefficients are listed in Table I. It is easy to verify that the fourth order method G_h^4P is time-symmetric, as $G_h^4P\circ G_{-h}^4P(\mathbf{z})\equiv\mathbf{z}$ holds for any $\mathbf{z}$. Because χ_h is volume-preserving, the method G_h^4P is volume-preserving.

TABLE I. Composition coefficients of the processed method G_h^4P.

$a_1 = \frac{\sqrt{18069}-15}{300}$	$b_1 = \frac{6}{25}$
$a_2 = \frac{9}{25}$	$b_2 = -\frac{\sqrt{18069}+15}{300}$
$a_3 = b_2, a_4 = b_1$	$b_3 = a_2, b_4 = a_1$
$x_1 = 0$	$y_1 = 0.1171835753202670$
$x_2 = 0.4731269439352653$	$y_2 = -0.1351671439946886$
$x_3 = 1.350298160490375$	$y_3 = -0.4530449481299280$
$x_4 = 0.05719279780976250$	$y_4 = -0.1930850894788554$

III. LINEAR STABILITY ANALYSIS

It is well known that the stability analysis of a numerical scheme applied to arbitrary ordinary differential equations is of great complexity, so in this work, we restrict ourselves to linear problems. The linear stability result of a numerical method serves as a necessary condition for its stability in the case with nonlinear terms. The linear stability of the SVP methods applied to the non-relativistic dynamics has been analyzed in Ref. 13. In this section, we generalize this study to relativistic dynamics. In order to do this, we first present the linear test model equation.

We linearize the system (1) around a fixed point $(\mathbf{x}_0, \mathbf{p}_0) \in \mathbb{R}^6$. After a proper affine transformation, we consider the following approximate system as the test model:

$$\dot{\mathbf{x}} = \frac{1}{\gamma_0}\mathbf{p}, \quad \dot{\mathbf{p}} = -\frac{1}{B_0 c}\nabla\phi(\mathbf{x}) + \frac{\mathbf{p}}{\gamma_0} \times \frac{\mathbf{B}}{B_0}, \tag{12}$$

where $\mathbf{B} = B_0\omega\mathbf{e}_z$ corresponds to the 0-th order truncation of the $\mathbf{x}$-expansion of the magnetic field, and

$$\phi(\mathbf{x}) = \frac{1}{2}\frac{qB_0^2}{m_0}\epsilon\left(\lambda_x^2 x^2 + \lambda_y^2 y^2 - \left(\lambda_x^2 + \lambda_y^2\right)z^2\right),$$
$$\lambda_x, \lambda_y > 0, \epsilon = \pm 1,$$

corresponds to the 2-nd order truncation of the expansion of the electric potential. The variables are dimensionless normalized by $l_0 = m_0 c/(eB_0)$ in space and $(\omega_{ce})^{-1} = m_0/(qB_0)$ in time, and $\gamma_0 = \sqrt{1+p_0^2} > 1$ is a constant. In the linearized system (12), the transverse motion and the axial dynamics are decoupled. As the SVP methods developed in this paper simulate this axial motion exactly, we only need to concentrate on its transverse motion. We consider the case with $\lambda^2 = \lambda_x^2 = \lambda_y^2$. Denote $\mathbf{x} = [x, y]$, $\mathbf{p} = [p_x, p_y]$, the two-degree test system is

$$\dot{\mathbf{x}} = \frac{1}{\gamma_0}\mathbf{p}, \quad \dot{\mathbf{p}} = -\epsilon\lambda^2\mathbf{x} + \frac{\omega}{\gamma_0}J\mathbf{p}, \tag{13}$$

where $J = \begin{pmatrix} 0 & 1 \\ -1 & 0 \end{pmatrix}$ is the standard symplectic matrix.

Applying the SVP methods with time step h to the test system (13), we derive

$$\begin{pmatrix} \gamma_0\mathbf{x}^{k+1} \\ h\mathbf{p}^{k+1} \end{pmatrix} = M\left(\epsilon\left(\frac{h\lambda}{\sqrt{\gamma_0}}\right)^2, \frac{h\omega}{\gamma_0}\right)\begin{pmatrix} \gamma_0\mathbf{x}^k \\ h\mathbf{p}^k \end{pmatrix}, \tag{14}$$

where M is the corresponding update matrix depending on $\epsilon(h\lambda/\sqrt{\gamma_0})^2$ and $h\omega/\gamma_0$. For the SVP methods constructed based on the splitting method in Eq. (3), the update matrix M is the product of update matrices for each subsystem. For the second order method $G_h = \phi_{h/2}^{F_1} \circ \phi_{h/2}^{F_2} \circ \phi_h^{F_3} \circ \phi_{h/2}^{F_2} \circ \phi_{h/2}^{F_1}$ in Eq. (6) applied to the test system (13), M is expressed as

$$M_s(h) = M_s^1(h/2)M_s^2(h/2)M_s^3(h)M_s^2(h/2)M_s^1(h/2), \tag{15}$$

where $M_s^1(h/2) = \begin{bmatrix} I & h/2I \\ \mathbf{0} & I \end{bmatrix}$, $M_s^2(h/2) = \begin{bmatrix} I & \mathbf{0} \\ -\epsilon h^2\lambda^2/(2\gamma_0)I & I \end{bmatrix}$, and $M_s^3(h) = \begin{bmatrix} I & \mathbf{0} \\ \mathbf{0} & O(h\omega/\gamma_0) \end{bmatrix}$ are four-dimensional matrices, and $O(h\omega)$ is a rotation matrix $O(a) = \begin{bmatrix} \cos(a) & \sin(a) \\ -\sin(a) & \cos(a) \end{bmatrix}$. If we replace $h\omega$ with $2\arctan(h\omega/2)$ in Eq. (15), we can get the evolution matrix of the method $\tilde{G}_h^2$ in Eq. (7).

It has been presented that a volume-preserving method applied to a source free system is linearly stable if and only if the eigenvalues of the update matrix have modulus 1.[13] In Fig. 1, we display the stability domains of the second order volume-preserving methods with respect to $\epsilon h\lambda/\sqrt{\gamma_0}$ and $h\omega/(\gamma_0\pi)$, where the left bottom region of the blue dashed line indicates the physically unstable region of the test system.

From the observation of Fig. 1, we get the following results:

(1) When $\epsilon = 1$, both of the two schemes are stable if $h\lambda/\sqrt{\gamma_0} < 2$, i.e., $h < 2\sqrt{\gamma_0}/\lambda$. This means that if γ_0 is large or λ is small, the larger h can be taken to guarantee that the second order SVP methods are still linearly stable. It is noticed that larger $\gamma_0 = \sqrt{1+p_0^2}$ implies larger kinetic energy.
(2) If the two schemes $\tilde{G}_h^2$ and G_h^2 are applied to a problem with uniform electric field, i.e., $\lambda = 0$, they are unconditionally stable. Moreover, for the case when the electric field changes slowly in space, i.e., λ is small enough, the schemes $\tilde{G}_h^2$ and G_h^2 can be stable for a very large h. In practical computation, due to the Nyquist limit, we need the time step h satisfying $h\omega/(\gamma_0\pi) \le 1$ in order to accurately simulate the Larmor cyclotron.
(3) From the two plots in Fig. 1, it is observed that the stability domain of the method G_h^2 is 2π periodic with respect to $h\omega/\gamma_0$, while for the method $\tilde{G}_h^2$, the domain becomes larger along with the increasing $h\omega/\gamma_0$ in $[0, 5\pi]$. It is known that the slope of the line across the origin of coordinate is $s = \omega/(\sqrt{\gamma_0}\pi\lambda)$. With λ, ω, and γ_0 satisfying $s < 0.52$, the stability domain shown in Fig. 1 implies that the method G_h^2 allows a larger time step than one for the method $\tilde{G}_h^2$.

In Fig. 2, the stability of the fourth order method G_h^4P in Eq. (11) is compared with the composed methods G_h^4Y in Eq. (8) and G_h^4S in Eq. (9). It is observed that compared with the second order method G_h^2 in Fig. 1(a), the fourth order Suzuki composition G_h^4S has an enlarged stability domain in Fig. 1(b), while the Yoshida composition has a shrunk stability domain in Fig. 1(a). Among the three methods, the processed method G_h^4P has the largest stability domain shown in Fig. 1(c). This verifies that the processed method allows both

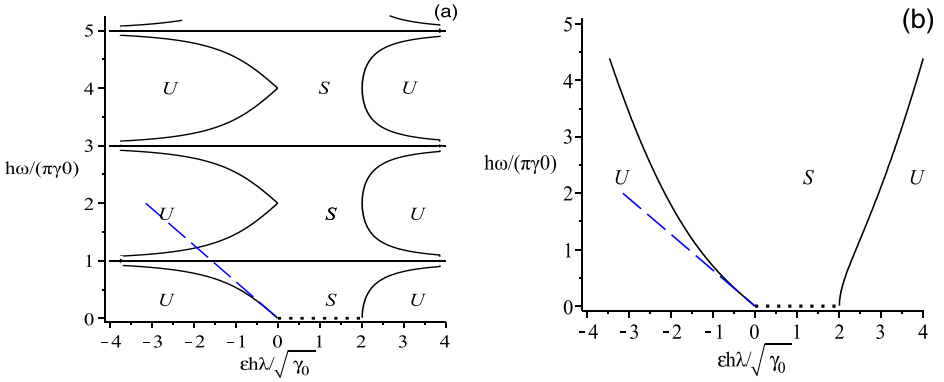

FIG. 1. Stability domains of second order volume-preserving numerical methods. Left: the method G_h^2 in Eq. (6); right: the method $\tilde{G}_h^2$ in Eq. (7). The abscissa represents $\epsilon h\lambda/\sqrt{\gamma_0}$, and the ordinate represents $h\omega/(\gamma_0\pi)$. Here, λ^2 reflects the dimensionless value $\mathbf{E}(\mathbf{x}_0)/B_0c$, ω reflects the dimensionless value $B(\mathbf{x}_0)/B_0$, and $\gamma_0 = \sqrt{1+p_0^2}$. The solid curves are boundaries of the stability domain. "S" labels stable region, "U" labels unstable region. The left bottom region below the dashed line $\omega = -2\epsilon\lambda\sqrt{\gamma_0}$ is the unstable region of the test system.

higher order of accuracy and larger threshold of the time step h.

We have studied the test equations that are linear and time-independent. To derive stronger stability conditions, we can also set the fields in the test model to be time-dependent, with $\lambda(t)$ and $\omega(t)$ being two functions depending on the time. Then the stability domain can be determined by analyzing the norm of the following stability matrix:

$$M\left(\epsilon\left(\frac{h\lambda(t_0+c_1h)}{\sqrt{\gamma_0}}\right)^2, \frac{h\omega(t_0+c_1h)}{\gamma_0}, \ldots, \epsilon\left(\frac{h\lambda(t_0+c_sh)}{\sqrt{\gamma_0}}\right)^2, \frac{h\omega(t_0+c_sh)}{\gamma_0}\right),$$

where $c_1 = 1/2$ for the 2nd order SVP algorithm, and $c_{2j-1} = a_j, c_{2j} = b_j, j = 1\ldots,4$ for the processed method G_h^4P. The more general stability analysis will be studied in our future work.

IV. NUMERICAL EXPERIMENTS

In this section, the SVP methods presented above are applied to simulate relativistic problems with different electromagnetic fields.

Example 1. Consider the relativistic dynamics of a charged particle in the Penning trap. For this problem, the electromagnetic field is given by

$$\mathbf{B} = B_0\mathbf{e}_z, \quad \mathbf{E} = -\epsilon E_l\left(\frac{x}{R_0}\mathbf{e}_x + \frac{y}{R_0}\mathbf{e}_y\right),$$

where $B_0 = 1\,\mathrm{T}$, $E_l = 3\,\mathrm{V/m}$, and $R_0 = 1\,\mathrm{m}$.

We first simulate the relativistic dynamics of an electron in the ideal penning trap with $\epsilon = 1$. We take the initial momentum as $\mathbf{p}_{0\parallel} = 0.1m_0c$, $\mathbf{p}_{0\perp} = 0.5m_0c$, and the initial position as $\mathbf{x} = 0.3l_0\mathbf{e}_x - l_0\mathbf{e}_y$. After normalizing the temporal variables by $T_0 = m_0/(eB_0) = 5.7 \times 10^{-12}\,\mathrm{s}$ and the spatial variables by $l_0 = m_0c/(eB_0)$, the dimensionless field parameters are (N denotes the normalized variable)

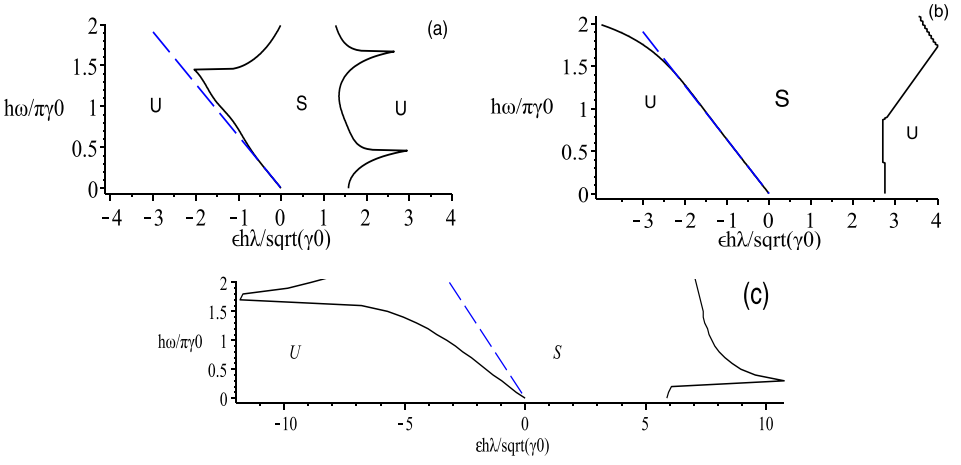

FIG. 2. Stability domain of the fourth order volume-preserving methods. (a) The Yoshida composition based on the method G_h^2. (b) The Suzuki composition method based on G_h^2. (c) The processed fourth order method G_h^4P. Here, λ, ω, and γ_0 are defined as above.

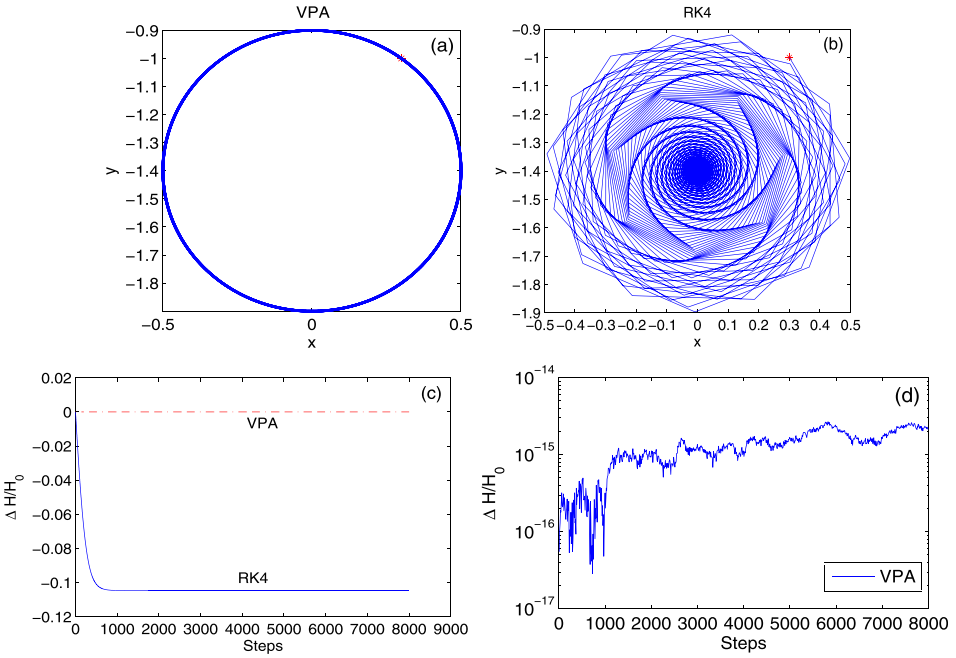

FIG. 3. The simulation result of the relativistic dynamics of a particle in an ideal penning trap. The SVP methods and RK4 are iterated for 8000 steps with the step size $h = 0.3\pi$. (a) Orbit by the SVP methods. (b) Orbit by RK4. (c) and (d) Energy error as a function of steps.

$$\mathbf{B}_N = \omega \mathbf{e}_z, \quad \mathbf{E}_N = -\lambda^2 \left(\frac{x}{R_0} \mathbf{e}_x + \frac{y}{R_0} \mathbf{e}_y \right),$$

$$\text{with } \omega = 1, \lambda = 10^{-4}.$$

In this experiment, as the initial kinetic energy is bounded and close to 1, we choose $\gamma_0 = 1$ in the test equation (13). As $\epsilon = 1$, and the slope $s = \omega/(\lambda\sqrt{\gamma_0}\pi) = 10^4/\pi$ is large enough, from Fig. 1, we can see that the two second order SVP methods G_h^2 and $\tilde{G}_h^2$ are stable regardless of h. Thus, the step size should be chosen in $h \le \gamma_0 \pi/\omega = \pi$ according to the Nyquist limit.

In Fig. 3, we show the numerical results computed by the SVP methods running over 8000 steps with $h = 0.3\pi = 5.37 \times 10^{-12}$ s. The explicit fourth order Runge-Kutta method RK4 is calculated as a comparison. First, RK4 has a larger computing expense than the second order SVP method, as the CPU time of the SVP method is 0.62 s, while that of RK4 is 0.96 s. It is known that the exact orbit of the particle is a nearly closed orbit with radius $p_\perp/(m_0 c) \approx 0.5$. It is observed from Fig. 3(a) that the SVP method can simulate the orbit well. The relative energy error displayed in Fig. 3(b) is bounded up to 10^{-14} during the entire simulation time. Conversely, Figs. 3(b) and 3(c) show that the numerical orbit spirals inside and the energy error is dissipating. This is because the numerical solution computed by RK4 is not stable for long term computations.

In Fig. 4, the global errors of the dimensionless position variables computed by the second and fourth order methods

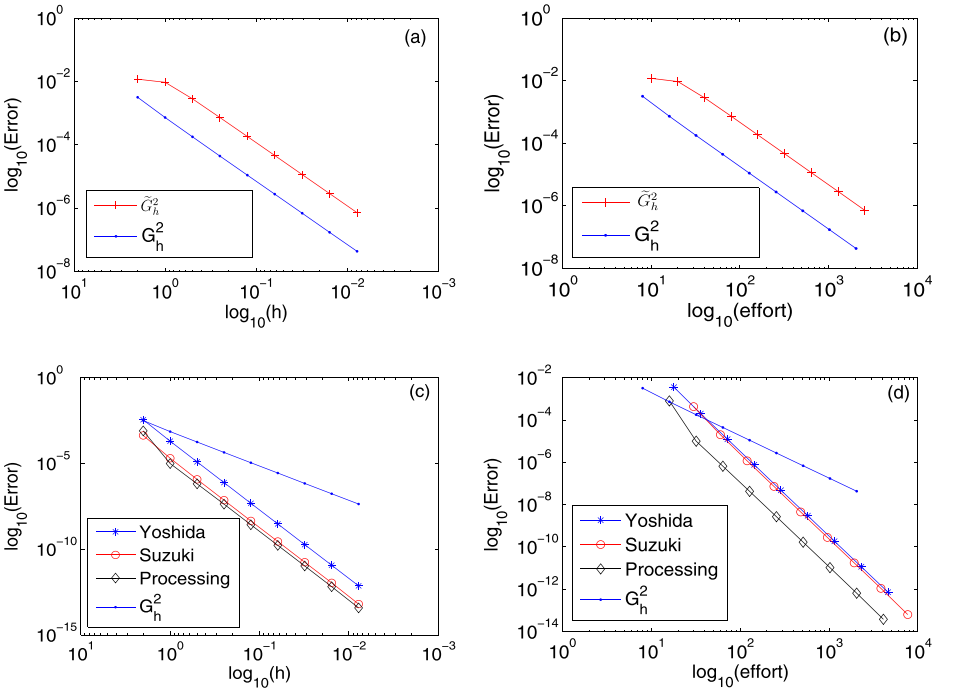

FIG. 4. Relative errors of the dimensionless position variables at the time $t = 20T_0$, in the experiment with an ideal penning trap. (a) and (c) Errors as a function of the time step h; (b) and (d) errors as a function of the computing effort (counted by evaluations of **E**). (a) and (b) Errors of the 2nd order methods; (c) and (d) errors of the 4-th order methods compared with the second order method G_h^2.

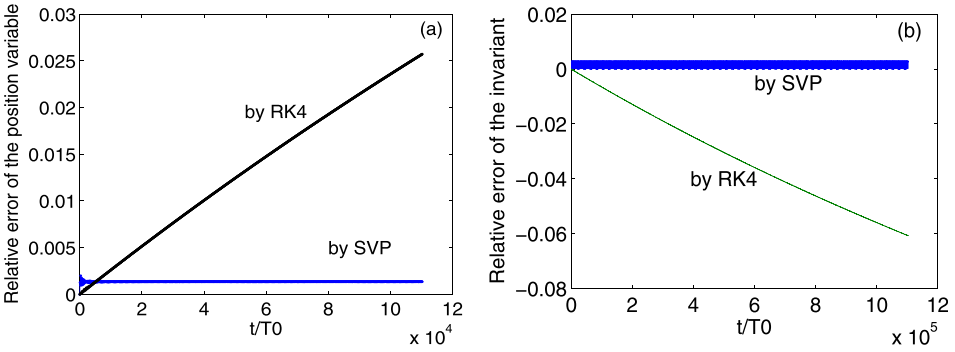

FIG. 5. The long-term simulation result of the relativistic dynamics of a particle under a plane polarized electromagnetic wave. The step size is $h = 0.1$. (a) Relative error of the position variables $\|\mathbf{x}_n - \mathbf{x}(nh)\|/\|\mathbf{x}(nh)\|$ as a function of normalized time t/T_0; (b) relative error of the invariant $I(t)$.

till the normalized time $t/T_0 = 20$ are compared. Figs. 4(a) and 4(c) display the errors as a function of time step h, which verifies the orders of the SVP methods. In Fig. 4(a), the method G_h^2 is more accurate than the method $\tilde{G}_h^2$ because of the smaller error constant. In Fig. 4(c), it is clear that the processed fourth order method is the most accurate. Figs. 4(b) and 4(d) display the errors as a function of the computing efforts, which are counted by the number of the evaluations of $\mathbf{E}$. It is observed that if the given tolerance on numerical errors is less than 0.01%, the fourth order methods need less computing efforts than the second order methods. Among the fourth order methods, the processed method $G_h^4 P$ is the cheapest.

Example 2. Now we study the long-term performances of the SVP methods in the case with time-dependent electromagnetic fields. The problem possessing a plane polarized electromagnetic wave (see Ref. 31) is considered. After normalizing the variables as before, we choose the dimensionless fields to be

$$\mathbf{E} = E_y \mathbf{e}_y, \quad \mathbf{B} = B_z \mathbf{e}_z, \quad E_y = B_z = 3\sin(3(t-x)).$$

In this case, the evolution of the particle energy $W(\mathbf{p})$ satisfies

$$I(t) = W(\mathbf{p}(t)) - p_x(t) = \text{constant},$$

where p_x represents the momentum in the x-direction. Setting the initial position and momentum to be $\mathbf{x}_0 = 0.3\mathbf{e}_x + 0.2\mathbf{e}_y$, $\mathbf{p}_0 = 0.4\mathbf{e}_x + 0.3\mathbf{e}_y + 0.1\mathbf{e}_z$, we run the second order SVP methods for 10^6 steps with the step size $h = 0.1$. The fourth order Runge-Kutta method is used as a comparison. During the entire simulation, the CPU time of the SVP method is 0.20 s, while the CPU time of RK4 is up to 0.24 s. The results are shown in Fig. 5. From Fig. 5(a), we can see that the relative error of RK4 is smaller than that of the SVP method at the beginning few steps, but it grows over 1% rapidly. Meanwhile, the relative error of SVP methods stays below 0.5% over the entire simulation time. In Fig. 5(b), the invariant $I(t)$ is preserved approximately by the SVP method, while the invariant computed by RK4 is dissipated. It can be verified that for the long-term simulation, the two second order SVP methods are linearly and nonlinearly stable.

V. CONCLUSION

We have constructed explicit high order volume-preserving methods for the relativistic dynamics of a charged particle by the splitting technique with processing. For the system with time-dependent fields, we reformulate the system by extending its dependent variables space to include the time t. With the newly derived system, we give a valid construction procedure of the symmetric volume-preserving methods. We have employed the processing technique to present efficient methods with high order of accuracy. Linear stability, which can serve as a hint on the choice of time step size of the SVP methods, has been analyzed. Numerical experiments show that the SVP methods are accurate and conservative for the long term tracking of the trajectory of relativistic particles. More efficient SVP methods as well as the advanced analysis of their nonlinear stability will be studied in our future work.

ACKNOWLEDGMENTS

This research was supported by the ITER-China Program (2015GB111003, 2014GB124005), the JSPS-NRF-NSFC A3 Foresight Program in the field of Plasma Physics (NSFC-11261140328), the National Science Foundation of China (11271357, 11575186, 11575185, 11505185, and 11505186), the Foundation for Innovative Research Groups of the NNSFC (11321061), and the Fundamental Research Funds for the Central Universities (WK2030040057).

[1]R. D. Ruth, IEEE Trans. Nucl. Sci. **30**, 2669 (1983).
[2]K. Feng, in *Proceedings of 1984 Beijing Symposium on Differential Geometry and Differential Equations*, edited by K. Feng (Science Press, 1985), pp. 42–58.
[3]K. Feng and M. Qin, *Symplectic Geometric Algorithms for Hamiltonian Systems* (Springer-Verlag, 2010).
[4]E. Hairer, C. Lubich, and G. Wanner, *Geometric Numerical Integration: Structure-Preserving Algorithms for Ordinary Differential Equations* (Springer, New York, 2003).
[5]Z. Shang, Numer. Math. **83**, 477–496 (1999).
[6]H. Qin and X. Guan, Phys. Rev. Lett. **100**, 035006 (2008).
[7]H. Qin, X. Guan, and W. M. Tang, Phys. Plasmas **16**, 042510 (2009).
[8]H. Qin, S. Zhang, J. Xiao, J. Liu, Y. Sun, and W. M. Tang, Phys. Plasmas **20**, 084503 (2013).
[9]J. Squire, H. Qin, and W. M. Tang, Phys. Plasmas **19**, 084501 (2012).
[10]S. A. Chin, Phys. Rev. E **77**, 066401 (2008).
[11]J. M. Finn and L. Chacón, Phys. Plasmas **12**, 054503 (2005).
[12]Y. He, Y. Sun, J. Liu, and H. Qin, J. Comput. Phys. **281**, 135 (2015).
[13]Y. He, Y. Sun, J. Liu, and H. Qin, J. Comput. Phys. **305**, 172 (2016).
[14]R. Zhang, J. Liu, H. Qin, Y. Wang, Y. He, and Y. Sun, Phys. Plasmas **22**, 044501 (2015).
[15]J. Xiao, J. Liu, H. Qin, and Z. Yu, Phys. Plasmas **20**, 102517 (2013).
[16]M. Kraus, "Variational integrators in plasma physics," Ph.D. thesis, Technical University of Munich, 2014.
[17]Y. Zhou, H. Qin, J. W. Burby, and A. Bhattacharjee, Phys. Plasmas **21**, 102109 (2014).

[18]B. A. Shadwick, A. B. Stamm, and E. G. Evstatiev, Phys. Plasmas **21**, 055708 (2014).
[19]E. Evstatiev and B. Shadwick, J. Comput. Phys. **245**, 376 (2013).
[20]H. Qin, J. Liu, J. Xiao, R. Zhang, Y. He, Y. Wang, Y. Sun, J. W. Burby, L. Ellison, and Y. Zhou, Nucl. Fusion **56**, 014001 (2016).
[21]J. Xiao, H. Qin, J. Liu, Y. He, R. Zhang, and Y. Sun, Phys. Plasmas **22**, 112504 (2015).
[22]Y. He, Y. Sun, Z. Zhou, J. Liu, and H. Qin, e-print arXiv:1509.07794.
[23]J. Qiang, M. Furman, and R. Ryne, J. Comput. Phys. **198**, 278 (2004).
[24]K. Feng and Z. Shang, Numer. Math. **71**, 451 (1995).
[25]S. Blanes, F. Casas, and A. Murua, SIAM J. Numer. Anal. **42**, 531 (2004).
[26]S. Blanes, F. Casas, and A. Murua, SIAM J. Sci. Comput. **27**, 1817 (2006).
[27]S. Blanes, F. Diele, C. Marangi, and S. Ragni, J. Comput. Appl. Math. **235**, 646 (2010).
[28]R. I. McLachlan and G. R. W. Quispel, Acta Numer. **11**, 341 (2002).
[29]H. Yoshida, Phys. Lett. A **150**, 262 (1990).
[30]M. Suzuki, Phys. Lett. A **165**, 387 (1992).
[31]E. M. McMillan, Phys. Rev. **79**, 498 (1950).